

## Effects of radiation quality on interactions between oxidative stress, protein and DNA damage in *Deinococcus radiodurans*

Igor Shuryak · David J. Brenner

Received: 13 January 2010 / Accepted: 1 June 2010  
© Springer-Verlag 2010

**Abstract** Ionizing radiation damages DNA and also induces oxidative stress, which can affect the function of proteins involved in DNA repair, thereby causing repair of DNA damage to become less efficient. We previously developed a mathematical model of this potentially synergistic relationship and applied it to  $\gamma$ -ray exposure data on the radiation-resistant prokaryote *Deinococcus radiodurans*. Here, we investigate the effects of radiation quality on these processes by applying the model to data on exposures of *D. radiodurans* to heavy ions with linear energy transfer (LET) of 18.5–11,300 keV/ $\mu$ m. The model adequately describes these data using three parameters combinations: radiogenic DNA damage induction, repair protein inactivation and cellular repair capacity. Although statistical uncertainties around best-fit parameter estimates are substantial, the behaviors of model parameters are consistent with current knowledge of LET effects: inactivation cross-sections for both DNA and proteins increase with increasing LET; DNA damage yield per unit of radiation dose also increases with LET; protein damage per unit dose tends to decrease with LET; DNA and especially protein damage yields are reduced when cells are irradiated in the dry state. These results suggest that synergism between oxidative stress and DNA damage may play an important role not only during  $\gamma$ -ray exposure, but during high-LET radiation exposure as well.

### Introduction

Not only radiation dose, but also radiation type, is important for biological effects. For example, so-called clustered DNA damage, consisting of closely spaced DNA single- or double-strand breaks (SSBs or DSBs) and base damage, is induced much more efficiently by densely ionizing particle radiations than by sparsely ionizing photons and is usually more difficult for cells to repair (Asaithamby et al. 2008; Hada and Georgakis 2008; Pinto et al. 2002a; Terato et al. 2007; Tsuruoka et al. 2005; Xue et al. 2009). The density of ionizations per unit of track length is correlated with linear energy transfer (LET). Thus, LET has become a useful parameter for representing radiation quality, although other parameters (e.g., particle energy and atomic number) also contribute (Taguchi and Kojima 2005; Taguchi et al. 2009).

The yield of indirect oxidative damage due to reactive oxygen species (ROS) also varies with radiation type. As LET increases, more radicals are created per particle track, but they are produced in closer proximity to one another, thereby increasing the probability of interactions between them leading to their disappearance (Kreipl et al. 2009; Meesungnoen and Jay-Gerin 2005; Yamaguchi et al. 2005). Consequently, the yield per unit absorbed energy of some very reactive types of ROS such as OH radicals decreases with increasing LET, but the yield of less reactive ones such as  $H_2O_2$  increases with LET, reaches a maximum and then decreases (Kreipl et al. 2009; Meesungnoen and Jay-Gerin 2005). Some radicals like OH are predominantly produced from ionized and excited water molecules, whereas others like  $H_2O_2$  predominantly from reactions of other radicals during the chemical phase.

In the previous article (Shuryak and Brenner 2009), we focused on potential interactions between DNA-damage

I. Shuryak · D. J. Brenner (✉)  
Center for Radiological Research,  
Columbia University Medical Center,  
630 West 168th St., New York, NY 10032, USA  
e-mail: djb3@columbia.edu

I. Shuryak  
e-mail: ishuryak@gmail.com

repair and radiation-induced oxidative damage to proteins involved in the DNA repair process. When sensitive sites on repair-related proteins are oxidized by radiation-induced ROS, the function of these proteins is altered, which may impede correct repair of DNA damage such as DSBs, enhancing cell death and mutagenesis (Adams et al. 1979; Bisby et al. 1982; Culard et al. 2003; Daly 2009; Daly et al. 2007; Eon et al. 2001; Ghosal et al. 2005; Goodhead and Nikjoo 1987; Kowalczyk et al. 2008; Saha et al. 1992). We developed a simple mathematical model intended to investigate this potential synergistic relationship using data on *Deinococcus radiodurans* as an example. This organism is a convenient system to examine such effects because it can survive doses of several thousand Gy, which are also in the relevant range for severe protein oxidation (Culard et al. 2003, 2005; Daly 2006, 2009; Daly et al. 2007; Gillard et al. 2004, 2007), whereas most other cell types are killed at much lower doses.

The main model assumptions are shown in Fig. 1, reproduced from the previous article (Shuryak and Brenner 2009). The model was consistent with the observed patterns of cell survival for this organism after chronic and acute exposures to low-LET  $\gamma$ -radiation. Here, we investigate the effects of radiation quality on the interactions between oxidative stress and DNA damage by applying the same model to survival data for *D. radiodurans* after acute exposures to high-LET radiation:  $\alpha$ -particles and heavy

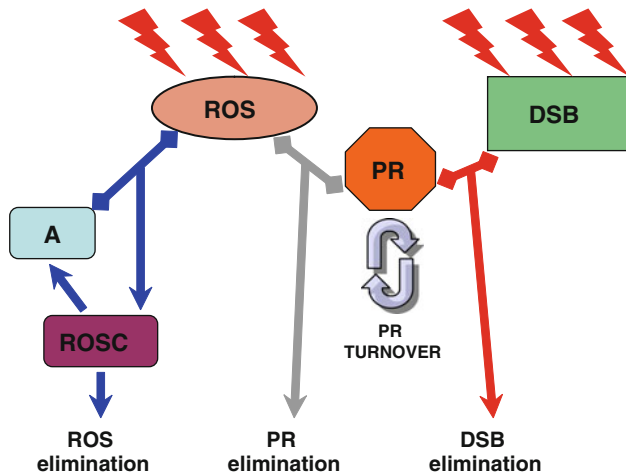


**Fig. 1** Schematic representation of model assumptions: Radiation (lightning symbols) produces reactive oxygen species (ROS) and DNA double-strand breaks (DSB). ROS can react with antioxidants (A) to form a complex (ROSC), which then decays, resulting in elimination of ROS and regeneration of the antioxidants. DSBs are eliminated by repair involving specific proteins (PR), which are produced and degraded at a certain turnover rate. Importantly, ROS can damage these proteins, resulting in diminution of their repair capacity. Consequently, those ROS that are not removed by antioxidants damage DNA repair machinery and hinder correct repair of DSBs. The figure is reproduced from reference Shuryak and Brenner (2009)

ions, spanning a range of LET of approximately 18.5–11,300 keV/ $\mu\text{m}$ .

For acute irradiation, the formalism can be greatly simplified, describing cell survival by only three parameter combinations: (1) the yield of radiation-induced DNA damage (e.g., DSBs) causing cell death, (2) the radiation inactivation constant for DNA repair proteins and (3) the cellular repair capacity (the combination of DNA repair rates, protein turnover rates and time available for repair). The patterns of variation of the first two of these parameters with radiation LET are analyzed; the third parameter is assumed not to depend on radiation. In general, these patterns are consistent with available knowledge of chemical and biological effects of high-LET radiations, suggesting that interactions between DNA damage and oxidative stress may play a substantial role at high LET as well as at low LET and that the mechanisms involved in these interactions can be modeled with tractable techniques.

## Materials and methods

### Mathematical description of cell survival after acute irradiation

According to the assumption that a single DSB that remains unrepaired by the time when the cell needs to proceed with DNA replication is potentially lethal, the predicted cell survival probability after high dose rate irradiation (i.e., when the irradiation time is short compared with the characteristic DSB repair time) is defined as  $S = \exp(-\text{DSB}[T_{\text{rep}}])$ , where  $T_{\text{rep}}$  is time available for repair and  $\text{DSB}(t)$  was calculated using equations 7 and 9 in the previous article (Shuryak and Brenner 2009). These equations are repeated here, now labeled (1):

$$\begin{aligned} \text{PR}_d &= c_5 \left( 2c_2c_3c_6/Y_2 + c_7 \left[ Y_1^{1/2} + c_2X_1 - c_3c_4 \right] \right) \\ &\quad \times Y_2 / (c_6[c_7Y_1^{1/2} + c_7\{c_2X_1 - c_3c_4\} + 2c_2c_3c_6]), \\ \text{where } X_1 &= c_1R - c_4A_{\text{tot}}, \\ Y_1 &= c_4^2(c_2A_{\text{tot}} + c_3)^2 + 2c_1c_2c_4R(c_3 - c_2A_{\text{tot}}) + (c_1c_2R)^2, \\ Y_2 &= \exp \left( -D \left[ c_7Y_1^{1/2} + c_2\{2c_3c_6 + c_7X_1\} - c_3c_4c_7 \right] \right) / \\ &\quad [2c_2c_3R] \Bigg) \\ \text{DSB}(t) &= c_8 D \exp(-c_9[c_6\{c_5t + \text{PR}_d\} \\ &\quad + \{c_5 - c_6\text{PR}_d\} \exp\{-c_6t\} - c_5]/c_6^2) \end{aligned} \quad (1)$$

Here,  $\text{PR}_d$  is the concentration of active repair proteins just after irradiation with a constant dose rate  $R$  up to total

**Table 1** Interpretations for all model parameters

Parameter	Interpretation	Units
$c_1$	ROS production by radiation	Concentration $\times$ dose $^{-1}$
$c_2$	ROS removal by antioxidant	Concentration $^{-1} \times$ time $^{-1}$
$c_3$	ROS removal by first-order kinetics	Time $^{-1}$
$c_4$	Regeneration of active antioxidant	Time $^{-1}$
$c_5$	Repair-protein production	Concentration $\times$ time $^{-1}$
$c_6$	Repair-protein degradation	Time $^{-1}$
$c_7$	Repair-protein inactivation by ROS	Concentration $^{-1} \times$ time $^{-1}$
$c_8$	DSB induction by radiation	Dose $^{-1}$
$c_9$	DSB repair	Concentration $^{-1} \times$ time $^{-1}$
$A_{\text{tot}}$	Total antioxidant concentration	Concentration
$T_{\text{rep}}$	Time available for DSB repair	Time

dose  $D$ , and interpretations for the parameters  $c_1$  to  $c_9$  and  $A_{\text{tot}}$  are provided in Table 1.

For acute irradiation, where the dose rate  $R$  approaches infinity, (1) can be greatly simplified, giving the following formula for cell survival:

$$S = \exp(-c_8 D \exp[-k_2 \{k_3 + (1 - \exp[-k_3]) \times (\exp[-k_1 D] - 1)\}]) \quad (2)$$

Here,  $k_1 = c_1 c_7/c_3$  (units = dose $^{-1}$ ),  $k_2 = c_5 c_9/c_6^2$  (dimensionless) and  $k_3 = c_6 T_{\text{rep}}$  (dimensionless). Behaviors of (2) in some limiting cases, such as complete absence of DSB repair, are explored in the “Appendix”.

For relatively small values of  $k_3$  (e.g.,  $< 1$ ), which are plausible based on our earlier results (Shuryak and Brenner 2009), the term  $1 - \exp[-k_3]$  is approximately equal to  $k_3$ . This allows (2) to be further simplified and one parameter to be eliminated by introducing  $k_{23} = k_2 k_3$ :

$$S = \exp(-c_8 D \exp[-k_{23} \exp\{-k_1 D\}]) \quad (3)$$

Therefore, according to (3), cell survival depends mainly on three parameter combinations (also listed in Table 2): (1) DSB induction by radiation ( $c_8$ , units = dose $^{-1}$ ), (2) repair protein inactivation by radiation ( $k_1$ , units = dose $^{-1}$ ) and (3) generalized DSB repair capacity of the cell ( $k_{23}$ , dimensionless). Only the first two of these are assumed to be radiation related ( $c_8$  and  $k_1$ ); the third depends on culture conditions and cell properties (e.g., genetic background, exponential or stationary phase of culture growth, type of growth medium, oxygenation), but not on radiation (although different radiation types can produce different types of DSBs, this is neglected here for model simplicity).

Because in this paper we analyze radiation effects not only in terms of dose ( $D$ , kGy), but also in terms of fluence ( $F$ , number of ion tracks per  $\mu\text{m}^2$ ), we define the radiation-related parameters  $c_8'$  and  $k_1'$  for fluence data. The corresponding formula for these fluence-related parameters is:

$$S = \exp(-c_8' F \exp[-k_{23} \exp\{-k_1' F\}]) \quad (3')$$

Because under the conditions used in the experimental data analyzed here *D. radiodurans* typically grows as 4-cell clusters, the survival for colony-forming units ( $S_{\text{cfu}}$ ) is the following function of cell survival:

$$S_{\text{cfu}} = 1 - (1 - S)^4 \quad (4)$$

This expression in (4) was fitted to the experimental data as described elsewhere.

#### Data sets and model fitting procedure

Here, three data sets (Dewey 1969; Imamura et al. 2002; Zimmermann et al. 1994) on survival of *D. radiodurans* after acute exposure to high-LET  $\alpha$ -particles and heavy ions were analyzed. These data sets contain a total of 19 survival curves: 15 for irradiation of cells in physiological state and 4 for irradiation in the dry state. Radiation doses were reported either in kGy (1 kGy = 1,000 Gy) or in particle fluence ( $\mu\text{m}^{-2}$ ). We converted between these units using the relationship  $D = F \times 1.602 \times 10^{-4}$  LET, where  $D$  is dose in kGy,  $F$  is ion fluence ( $\mu\text{m}^{-2}$ ), LET is in keV/ $\mu\text{m}$ , and assuming a target density of 1.0 g/cm $^3$ . When LET was not reported directly, approximate values were calculated for ions with the same energy and atomic number using the publically available software Energy-LET-Range Calculator v1.10.

The model parameter  $k_{23}$ , which was assumed to depend on experimental conditions but not on radiation type, was kept in common for all survival curves within each experimental set (i.e., for all data from the same reference). However, its value was allowed (and expected) to differ between experiments (Table 3), for example because some authors (Dewey 1969) irradiated wild-type *D. radiodurans* in exponential growth phase, others (Zimmermann et al. 1994) irradiated wild-type *D. radiodurans* in stationary phase, which is known to be more radiosensitive (Sukhi et al. 2009), and others (Imamura et al. 2002) used different strains of this bacterium.

The remaining radiation-related parameters  $c_8$  and  $k_1$  were adjusted without constraints for each survival curve (i.e., for each type of radiation). Fitting was performed using a customized random-restart simulated annealing algorithm implemented in the FORTRAN programming language by minimizing the squared differences between logarithms (base 10) of the data points (surviving fractions

**Table 2** The main parameter combinations, which determine cell survival after acute irradiation

Parameter	Definition	Units	Interpretation
$c_8$	$c_8$	Dose $^{-1}$	DSB induction by radiation
$k_1$	$c_1 c_7/c_3$	Dose $^{-1}$	Repair-protein inactivation by radiation
$k_{23}$	$c_5 c_9 T_{\text{rep}}/c_6$	None	Cellular repair capacity

for colony-forming units) and  $S_{\text{cfu}}$  predictions from (4). Logarithms were used to give more weight to small surviving fractions (e.g., 0.1, 0.01), which typically determine survival curve shape to a greater extent than surviving fractions near unity.

Statistical uncertainties around the best-fit parameter values were estimated by generating multiple synthetic data sets for each survival curve by assuming that the logarithms of  $S_{\text{cfu}}$  are normally distributed and by fitting the model to each of these data sets. If the standard deviation corresponding to each data point was not provided in the source reference, it was assumed to be equal to 0.1 units on a logarithmic (base 10) scale.

## Results

Typical colony-forming unit ( $S_{\text{cfu}}$ ) survival curves for *D. radiodurans* after acute exposures to various types of high-LET radiation are shown in Fig. 2. The curves are characterized by an initial shoulder at low doses, where surviving fractions do not decline very much from unity, followed by a relatively abrupt transition to an exponential terminal slope at higher doses. This basic shape is the same as for low-LET  $\gamma$ -radiation (Daly et al. 2004; Shuryak and Brenner 2009), although the actual values for the extent of the shoulder and the terminal slope are of course modulated by radiation type. The preservation of the shoulder with increasing LET is an indication of very efficient DNA damage repair in *D. radiodurans* (although the presence of 4 cells per colony-forming unit also contributes to the shoulder in the curve), which (unlike many other cell types) apparently can effectively repair even clustered damage induced by high-LET radiations (Asaithamby et al. 2008; Hada and Georgakis 2008; Pinto et al. 2002a; Terato et al. 2007; Xue et al. 2009). This is consistent with current knowledge about DNA repair in this organism: repair is homology based (Blasius et al. 2008; Zahradka

**Table 3** Comparison of best-fit model predictions with the data

Ion	E (MeV/amu)	LET (KeV/ $\mu\text{m}$ )	D <sub>50</sub> (kGy)		D <sub>10</sub> (kGy)		D <sub>1</sub> (kGy)		Reference
			Data	Model	Data	Model	Data	Model	
He	10.0	18.5	8.65	9.06	12.2	12.2	16.3	16.3	D
Li	10.0	41.7	8.00	8.09	10.7	10.7	13.9	13.9	D
Li	5.0	72.0	7.70	6.97	8.80	8.85	11.1	10.9	D
C	~18.8	~100	3.90	4.09	6.39	6.25	9.20	9.25	Ip
B	10.0	115	7.70	7.07	8.80	8.90	10.7	10.8	D
C	10.0	165	7.54	7.91	10.0	9.89	11.8	11.9	D
He, Li	0.37, 0.12	~200	9.72	9.83	14.0	13.9	18.7	18.7	Ip
Ne	~16.8	~300	3.90	3.98	7.61	7.24	11.6*	11.8	Ip
O	10.0	290	8.10	8.75	10.9	10.9	13.0	13.0	D
Ne	10.0	444	8.67	10.0	12.6	12.6	15.4	15.3	D
Ar	10.5	1,240	4.50	4.84	9.00	8.72	13.8*	13.0	Z
Ar	10.0	1,280	15.5	16.3	20.3	20.0	23.2	23.4	D
Ar	4.1	2,010	8.96	9.64	16.1	16.0	23.6*	22.3	Z
Ni	9.5	2,700	4.55	4.51	8.39	8.30	12.8*	12.6	Z
Pb	11.4	11,300	3.81	3.49	5.81	5.58	8.51	8.30	Z
C	~18.8	~100	29.3	29.2	43.2	40.3	51.0*	50.8	Id
He, Li	0.37, 0.12	~200	26.6	27.7	—	38.3	—	48.2	Id
Ne	~16.8	~300	16.6	16.5	22.2	22.6	28.8	28.6	Id
O	~6.4	~400	10.5	13.2	17.7	18.4	25.3	24.1	Id

Approximate energies (E) and LET values are provided for each radiation type. D<sub>50</sub>, D<sub>10</sub> and D<sub>1</sub> represent radiation doses at which colony-forming unit surviving fraction equals 50, 10 and 1%, respectively. Values labeled “data” were estimated from the experimentally measured survival curves, sometimes by extending the terminal slope (in this case they are marked by asterisks). In this and the following tables, the label “He, Li” refers to particles generated from the boron capture neutron reaction (Imamura et al. 2002). References: D (Dewey 1969); I (Imamura et al. 2002), p irradiation in physiological state, d in dry state; Z (Zimmermann et al. 1994)

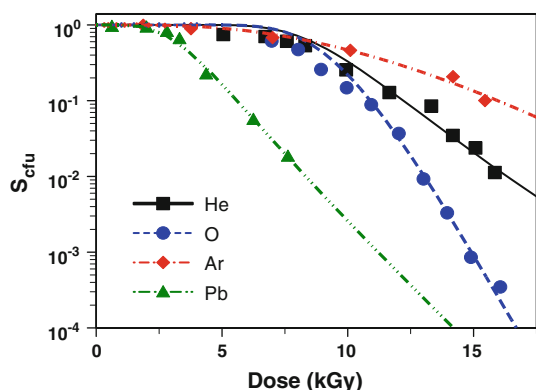


**Fig. 2** Typical *D. radiodurans* survival curves for acute irradiation with ions of different LET. The symbols are data points, and the lines are corresponding model fits using parameters in Tables 4, 5. Legend: black squares 4He2+ ions, LET = 18.5 keV/ $\mu$ m (Dewey 1969); blue circles 8O16+ ions, LET = 290 keV/ $\mu$ m (Dewey 1969); red diamonds 18Ar40+ ions, LET = 2,010 keV/ $\mu$ m (Zimmermann et al. 1994); green triangles 82Pb207+ ions, LET = 11,300 keV/ $\mu$ m (Zimmermann et al. 1994) (color figure online)

et al. 2006), utilizing multiple genome copies, and is in principle error free, resulting in essentially 100% cell survival and absence of mutagenesis up to certain doses (Schmid and Lidstrom 2002; Sukhi et al. 2009). Our model, which assumes very efficient repair as long as repair-related proteins remain functional, therefore provides a good conceptual and quantitative description of survival curve shape in *D. radiodurans* (Fig. 2). The similarity of model fits to the data for all survival curves, including those not shown in Fig. 2, can be assessed by comparing measured (estimated directly from the data) and predicted radiation doses yielding 50, 10 and 1% survival (Table 3).

Figure 3 shows in more detail the results of fitting the model function  $S_{\text{cfu}}$  from (4) to experimental survival curves, using the data from Zimmermann et al. (1994) as an example. The parameter  $k_{23}$ , which was simultaneously optimized for several survival curves from the same experimental set as discussed earlier, often exhibited a single, clearly defined deviance minimum (Fig. 3a, b). However, the deviance landscapes for  $c_8$  and  $k_1$ , which were optimized for each ion survival curve separately, contained several minima distributed along bands of  $c_8$  and  $k_1$  values (Fig. 3c–f). These bands containing minima result from the approximately compensatory relationship of  $c_8$  and  $k_1$ , e.g., see (3): numerically similar cell survival values can be generated by large  $c_8$  and small  $k_1$ , and vice versa.

The deepest of all available minima within a plausible parameter range was identified in each case, and the corresponding best-fit model parameters for all analyzed survival curves are provided in Tables 4, 5 and plotted in Fig. 4. Because there are often several minima which offer similar quality of fit, but differ substantially in location, best-fit parameter uncertainties can be large and

asymmetric (see 95% confidence intervals in Tables 4, 5). Although caution should be used when interpreting such results, some potentially useful generalizations can be made.

When expressed as an inactivation cross-section (i.e., in units of ion fluence $^{-1}$  =  $\mu$ m $^2$ ), the best-fit yield of DNA damage causing clonogenic cell death (parameter  $c_8'$ ) increases with LET with no evidence of saturation at high LET values. This trend is well described by the simple regression equation shown in Fig. 4a, where the logarithm of  $c_8'$  for cells irradiated in the physiological state increases linearly with the logarithm of LET with a slope somewhat >1. For the heaviest ions (Pb), the cross-section approaches the physical size of the *D. radiodurans* cell.

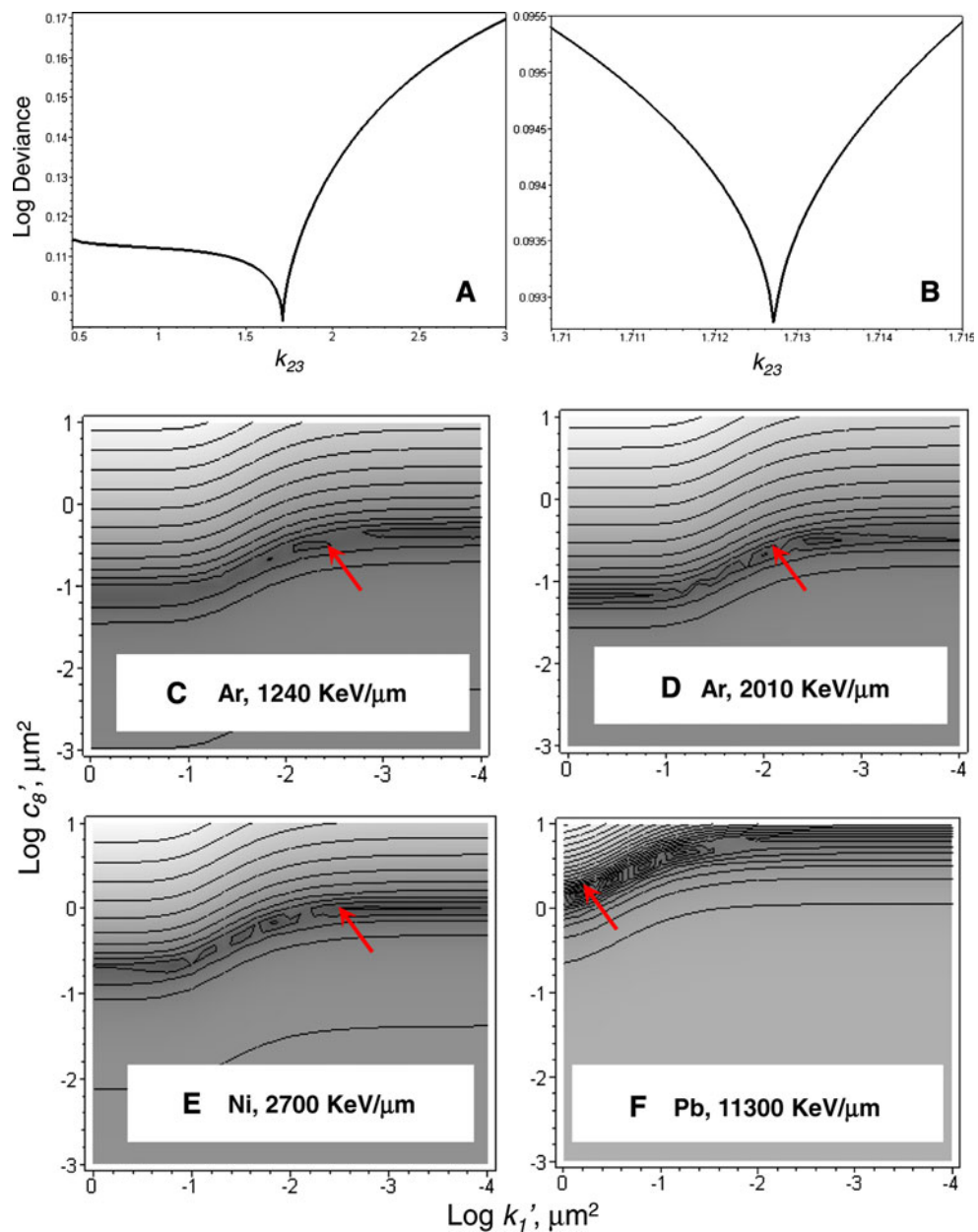
Interestingly,  $c_8'$  values can be greater than DSB induction values measured by PFGE: for example, the DSB induction value measured for Ni ions was about 0.13  $\mu$ m $^2$  (Zimmermann et al. 1994), and our best-fit estimate was 0.888 (95% confidence interval 0.187–1.81)  $\mu$ m $^2$  (Tables 4, 5). Perhaps, DSBs could have been undercounted by PFGE due to the presence of several closely spaced breaks induced by high-LET radiation (Pinto et al. 2002a, b; Terato et al. 2007), perhaps lesions other than DSBs, e.g., protein–DNA cross-links (Culard et al. 2005), contribute substantially to cell death in *D. radiodurans*, and/or perhaps additional DSBs are induced after radiation during repair of clustered DNA damage (D’Souza and Harrison 2003; Yang et al. 2006). Even more marked discrepancies between DSB induction and cell inactivation cross-sections were reported earlier for other bacteria (Micke et al. 1994).

It is also noteworthy that low energy neutrons used to generate  $\alpha$ -particles by boron capture did not have any effect on *D. radiodurans* survival at least up to a dose of 15 kGy (Imamura et al. 2002), whereas such neutrons are very effective at killing *E. coli* (same reference) and mammalian cells (Yamamoto et al. 2003), therefore suggesting that they do cause DNA damage. Perhaps, neutrons are not very effective at inactivating *D. radiodurans* repair proteins, which allows these proteins to retain their function at doses of 15 kGy or more, allowing the neutron-induced DNA damage to be repaired with few errors.

When parameter  $c_8$  is expressed per unit of radiation dose, the pattern of its LET dependence may suggest that DNA damage yield per unit dose initially rises with LET, but reaches a maximum and saturates above several hundred keV/ $\mu$ m (Tables 4, 5; Fig. 4c). A simple monotonic regression that assumes a linear dependence of the logarithm of  $c_8$  per unit dose on the logarithm of LET suggests a small positive slope (Fig. 4c). As expected,  $c_8$  is lower for cells irradiated in the dry state.

Repair protein inactivation per ion track (parameter  $k_1'$ ) also increases with LET, as shown by an increasing

**Fig. 3** Model fitting results to the data from reference (Zimmermann et al. 1994). Panel **a** shows a clear best-fit minimum for model deviance (for the sum of all four survival curves from the cited reference) for parameter  $k_{23}$ , and panel **b** magnifies the vicinity of this minimum. Panels **c–f** show the model deviance landscapes for each ion survival curve for parameters  $c_8$  and  $k_1$ , using the optimum value of  $k_{23} = 1.7127$ . The contours are iso-deviance values, and *darker shading* indicates decreasing deviance. Arrows mark the approximate locations of the deepest minima (for exact values see Tables 4, 5). Clearly, several minima occur for each survival curve within a band of  $c_8$  and  $k_1$  values, as discussed in the main text



cross-section (Tables 4, 5; Fig. 4b), which is approximately linear on a log–log plot. The rate of increase is slower than for  $c_8'$  and is  $<1$  (Fig. 4b). The magnitude of the cross-section for  $k_1'$  is usually lower than for DNA damage ( $c_8'$ ).

Expressed per unit dose,  $k_1$  tends to decrease with LET, showing a negative slope on a log–log plot (Fig. 4d). This decreasing trend is heavily influenced by the data set where seven ions had approximately the same energy of 10 meV/amu (Dewey 1969). Similarly to the behavior of DNA damage ( $c_8$ ), the protein inactivation parameter is lower for cells irradiated in the dry state.

As discussed in the “Methods” section, the parameter  $k_{23}$ , which represents cellular repair capacity and is not directly related to radiation, was kept in common for all

survival curves from the same reference, but varied between references because of variation in experimental conditions, cell growth phase and strain of *D. radiodurans* (Tables 4, 5). Given the parameters composing the combination  $k_{23}$  (see Tables 1, 2), the best-fit values listed in Tables 4 and 5 are consistent with biologically plausible protein turnover and DNA repair rates and time available for repair on the scale of several hours.

## Discussion

Ionizing radiation damages important biomolecules both by direct energy deposition and by producing a variety of

**Table 4** Best-fit model parameter values for different radiation types, for *D. radiodurans* cells irradiated in the physiological state

Ion	$10^3 \times c_8' (\mu\text{m}^2)$	$10^3 \times k_1' (\mu\text{m}^2)$	$c_8 (\text{kGy}^{-1})$	$k_1 (\text{kGy}^{-1})$	$k_{23}$
He	1.21 (0.70, 21.8)	0.756 (0.029, 1.14)	0.409 (0.237, 7.37)	0.255 ( $9.6 \times 10^{-3}$ , 0.39)	7.07 (3.58, 8.27)
Li	3.41 (3.23, 51.2)	1.79 (0.198, 1.87)	0.510 (0.483, 7.67)	0.268 (0.0296, 0.280)	
Li	9.71 (8.42, 33.0)	2.99 (2.26, 4.24)	0.842 (0.730, 2.86)	0.259 (0.196, 0.368)	
B	16.9 (16.2, 44.4)	4.50 (3.98, 4.96)	0.919 (0.878, 2.41)	0.244 (0.216, 0.269)	
C	24.5 (22.8, 68.7)	5.45 (4.31, 6.24)	0.928 (0.862, 2.60)	0.206 (0.163, 0.236)	
O	41.6 (34.2, 269)	8.41 (1.38, 14.0)	0.895 (0.737, 5.78)	0.181 (0.0296, 0.302)	
Ne	46.8 (25.5, 615)	12.1 (1.55, 13.6)	0.658 (0.358, 8.65)	0.170 (0.0218, 0.191)	
Ar	153 (118, 636)	16.5 (4.51, 19.3)	0.744 (0.574, 3.10)	0.0806 (0.022, 0.094)	
Ar	368 (136, 766)	3.22 (2.58, 90.3)	1.85 (0.685, 3.86)	0.0162 (0.013, 0.455)	1.71 (0.49, 1.87)
Ar	243 (115, 541)	7.26 (5.12, 370)	0.756 (0.357, 1.68)	0.0226 (0.016, 1.15)	
Ni	888 (187, 1,810)	5.55 (4.06, 264)	2.05 (0.432, 4.18)	0.0128 ( $9.4 \times 10^{-3}$ , 0.61)	
Pb	1,360 (1,120, 3,600)	819 (163, 870)	0.751 (0.619, 1.99)	0.452 (0.090, 0.481)	
C	10.7 (9.15, 153)	8.12 (0.30, 9.29)	0.666 (0.571, 9.57)	0.507 (0.019, 0.580)	3.14 (2.73, 26.4)
He, Li	12.6 (9.55, 98.4)	4.71 (0.91, 6.70)	0.392 (0.298, 3.07)	0.147 (0.028, 0.209)	
Ne	24.4 (19.7, 1,320)	42.6 (0.30, 369)	0.507 (0.409, 27.5)	0.887 ( $6.3 \times 10^{-3}$ , 7.67)	

The parameters are DSB induction by radiation (expressed per unit of radiation dose,  $c_8$ , and as an inactivation cross-section,  $c_8'$ ); repair protein inactivation by radiation (also expressed in both sets of units as  $k_1$  and  $k_1'$ , respectively); and cellular repair capacity ( $k_{23}$ ). The ranges in parentheses represent 95% confidence intervals

**Table 5** Best-fit model parameter values for different radiation types, for *D. radiodurans* cells irradiated in the dry state

Ion	$10^3 \times c_8' (\mu\text{m}^2)$	$10^3 \times k_1' (\mu\text{m}^2)$	$c_8 (\text{kGy}^{-1})$	$k_1 (\text{kGy}^{-1})$	$k_{23}$
C	4.87 (2.32, 1,550)	0.378 (0.087, 1.63)	0.304 (0.145, 96.6)	0.0236 ( $5.5 \times 10^{-3}$ , 0.10)	3.14 (2.73, 26.4)
He, Li	10.4 (2.25, 1,830)	0.785 (0.027, 248)	0.326 (0.0702, 57.2)	0.0245 ( $8.3 \times 10^{-4}$ , 7.74)	
Ne	23.3 (16.1, 72.1)	2.22 (1.73, 4.34)	0.484 (0.334, 1.50)	0.0463 (0.036, 0.090)	
O	22.6 (16.5, 242)	5.87 (0.788, 11.7)	0.352 (0.258, 3.77)	0.0916 (0.012, 0.183)	

The parameter interpretations are the same as in Table 4, and the ranges in parentheses represent 95% confidence intervals

reactive radicals (e.g., ·OH) (Goodhead 2006; Hirayama et al. 2009; Stadtman 1993). Most radicals are eliminated by scavengers quickly after the passage of an ionizing particle, but they can have sufficient time to react with DNA, proteins and other molecules located in close proximity to where the radicals have been formed (Jonah and Madhava Rao 2001; Mozumder 1999; Spinks and Woods 1990). As LET increases, a particle's ability to cause direct ionization increases and so does the number of radical molecules per particle track, but the yield of the most reactive radicals (such as ·OH) per unit radiation dose generally decreases (Butts and Katz 1967; Kiefer et al. 2002b; Kreipl et al. 2009; Meesungnoen and Jay-Gerin 2005; Stenerlow et al. 2002a; Taguchi and Kojima 2005; Taguchi et al. 2009; Yamaguchi et al. 2005; Yamashita et al. 2008).

These trends suggest that (1) the amount of DNA damage such as DSBs, which is generated by both direct and indirect radiation action, should increase with LET both as a function of particle fluence (i.e., the inactivation cross-section for DNA should increase) and as a function of

absorbed dose (Asaithamby et al. 2008; Barendsen 1994; Belloni et al. 2002; Hada and Georgakilas 2008; Hamada et al. 2006; Kiefer et al. 2002a, b; Micke et al. 1994; Roots et al. 1990; Stenerlow et al. 2002a, b; Takahashi et al. 1983; Terato et al. 2007; Tsuruoka et al. 2005; Ward 1990; Yokota et al. 2007); (2) the amount of protein damage, which is generated mainly by indirect radiation effects, should be (at least qualitatively) consistent with the behaviors of radical (e.g., ·OH) yields, i.e., it should increase with LET as a function of particle fluence, but it should decrease with LET as a function of absorbed dose (Adams et al. 1971, 1979; Appleby et al. 1985; Bisby et al. 1982, 1984; Butts and Katz 1967; Goodhead and Nikjoo 1987; Henriksen 1966; Kowalczyk et al. 2008; Montaner et al. 2007; Roots et al. 1985; Saha et al. 1992; Taguchi and Kojima 2005; Takahashi et al. 1983); (3) irradiating cells in the dry state should hinder indirect oxidative damage caused by diffusion of radiogenic oxidants to a greater extent than direct ionization, so dry conditions should offer substantial protection, particularly for proteins (Butts and Katz 1967; Henriksen 1966; Sagstuen et al. 2004).

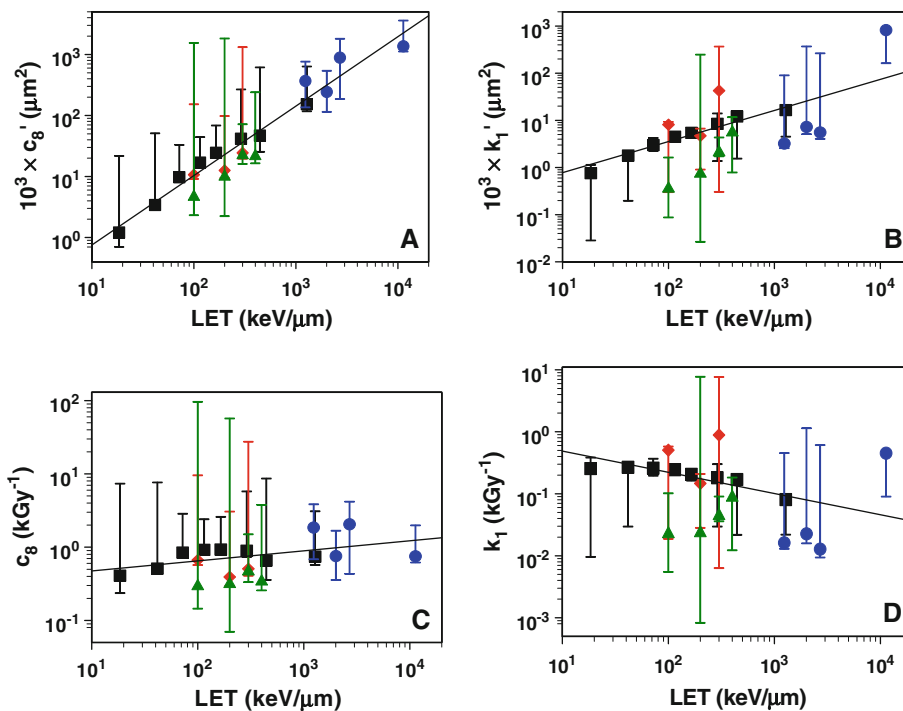


**Fig. 4** Best-fit values for DSB induction (parameter  $c_8$ ) and for repair protein inactivation (parameter  $k_1$ ) as function of LET. Both parameters are shown per unit of radiation dose ( $\text{kGy}^{-1}$ ) and as inactivation cross-sections ( $\mu\text{m}^2$ ). All points and error bars correspond to values in Tables 4, 5. Legend black squares (Dewey 1969); blue circles (Zimmermann et al. 1994); red diamonds (Imamura et al. 2002), irradiation in physiological state; green triangles (Imamura et al. 2002), irradiation in dry state. The lines represent best-fit regression equations with the form  $\log(y) = a + b \log(x)$ ,

where  $x$  is LET in  $\text{keV}/\mu\text{m}$ . The constants  $a$  and  $b$ , their 95% confidence intervals, and regression  $r^2$  values are panel **a** =  $-1.257$  ( $-1.624$ ,  $-0.890$ ),  $1.137$  ( $0.998$ ,  $1.277$ ),  $0.96$ ; panel **b** =  $-0.765$  ( $-1.774$ ,  $0.243$ ),  $0.658$  ( $0.275$ ,  $1.042$ ),  $0.51$ . For panels **c** and **d**, the  $r^2$  values are  $0.26$  and  $0.22$ , and the slopes  $b$  and their confidence intervals are, by definition, the same as in panels **a** and **b**, respectively, minus one. The four data points for irradiation of dry cells (green triangles) were not included in the regressions (color figure online)

Although there is considerable scatter in the points originating from different experiments, and the best-fit parameters have large statistical uncertainties, the behaviors of the radiation-related model parameters for DNA damage ( $c_8$ ) and protein damage ( $k_1$ ) are consistent with these expectations (Tables 4, 5; Fig. 4). Expressed as an inactivation cross-section,  $c_8'$  increases steadily with LET, and expressed per unit dose  $c_8$  also increases with LET and may saturate above several hundred  $\text{keV}/\mu\text{m}$  (Tables 4, 5; Fig. 4a, c). The data from Dewey (1969), where seven ions with the same energy but with different atomic number were used (Tables 4, 5), show a consistent decreasing trend of  $k_1$  per unit dose with increasing atomic number and hence with increasing LET (Fig. 4d). The only exception is the lightest ion, He, for which  $k_1$  is slightly below the corresponding value for Li. Also, comparing the results for C, He and Ne ion irradiation in the dry state and in the physiological state, Imamura et al. (2002) suggest that for dry cells  $c_8$  per unit dose is reduced only modestly, but  $k_1$  per unit dose is several-fold lower for dry cells than for hydrated ones (Tables 4, 5).

Despite its simplicity and limitations, the model presented here can potentially provide some insight into interactions between radiation-induced oxidative stress and DNA damage. Such interactions may be important not only for low-LET radiation, but also at much higher LET, and may need to be considered when predicting biological effects of high-LET exposures. The number of model parameters is relatively small (only three for acute exposures), and, as mentioned previously, the behaviors of these parameters as function of radiation type are generally consistent with current knowledge of oxidant yields and direct effects of high-LET particle radiations.

In principle, the model is not restricted to very high radiation doses, because radiogenic oxidative effects on DNA repair-related proteins are possible even at low doses, particularly if one considers not only protein inactivation, but more subtle modulations of function potentially leading to decreased repair fidelity and increased mutagenesis. For high-LET radiations, such as  $\alpha$ -particles, this may be particularly relevant because each ionizing track produces a dense pattern of energy deposition, which can be interpreted

as a high, but localized, radiation dose. Consequently, the same effects seen at high doses (high particle fluences) may be expected at lower doses/fluences, because the same types of ROS are created by radiation, only distributed more scarcely. In situations where important DNA repair- and regulation-related proteins are present in low copy number per cell, radiogenic damage to some of these molecules may have important effects which, along with DNA damage, contribute to biologically important endpoints such as mutagenesis and altered gene expression.

**Acknowledgments** Research supported by National Institutes of Health grants P41 EB002033-09 and P01 CA-49062.

## Appendix

In this appendix we explore some properties of the behavior of predicted cell surviving fraction after acute irradiation ( $S$ ), given by (3) of the main text. To do so, we apply some limiting cases described below.

### Effect of repair protein inactivation ( $k_1$ )

The model assumes that DSB repair in *D. radiodurans* is inherently 100% efficient, but that this efficiency is reduced by radiogenic inactivation of repair proteins (parameter  $k_1$ ), and also by limitations on protein turnover rates, repair rates, and time available for repair (affecting parameter  $k_{23}$ ). At relatively small radiation doses ( $D \ll 1/k_1$ ), most of the repair proteins remain functional and DSB repair remains very efficient. In this situation the term  $\exp[-k_1 D]$  in (3) is approximately equal to 1, so the cell-surviving fraction has the form:

$$S = \exp(-c_8 D \exp[-k_{23}]) \quad (5)$$

Here, the reduction of cell survival with dose is exponential, but this exponential slope is much smaller than the maximum it could reach (which would be equal to the DSB induction rate per unit dose,  $c_8$ ) by the factor  $\exp[-k_{23}]$ . The DSB repair efficiency could be approximated by  $1 - \exp[-k_{23}]$ .

In contrast, at much larger radiation doses ( $D \gg 1/k_1$ ), the term  $\exp[-k_1 D]$  in (3) approaches zero, so the cell surviving fraction becomes:

$$S = \exp(-c_8 D) \quad (6)$$

Consequently, at high doses the exponential slope approaches the DSB induction rate per unit dose ( $c_8$ ), meaning that efficiency of DSB repair is reduced essentially to zero.

### Effect of repair capacity ( $k_{23}$ )

If the repair-related parameter  $k_{23}$  approaches zero, e.g. due to genetic repair defects, the term  $\exp[-k_{23} \exp\{-k_1 D\}]$  in (3) becomes 1, and the exponential slope of the cell survival curve reaches the value  $c_8$ . In contrast, if  $k_{23}$  become large, this term becomes small, making the exponential slope  $\ll c_8$ , as intuitively expected.

## References

- Adams GE, Willson RL, Bisby RH, Cundall RB (1971) On the mechanism of the radiation-induced inactivation of ribonuclease in dilute aqueous solution. *Int J Radiat Biol Relat Stud Phys Chem Med* 20:405–415
- Adams GE, Posener ML, Bisby RH, Cundall RB, Key JR (1979) Free radical reactions with proteins and enzymes: the inactivation of pepsin. *Int J Radiat Biol Relat Stud Phys Chem Med* 35:497–507
- Appleby A, Christman EA, Jayko M (1985) Radiation chemistry of high-energy carbon, neon, and argon ions: hydroxyl radical yields. *Radiat Res* 104:263–271
- Asaithamby A, Uematsu N, Chatterjee A, Story MD, Burma S, Chen DJ (2008) Repair of HZE-particle-induced DNA double-strand breaks in normal human fibroblasts. *Radiat Res* 169:437–446
- Barendsen GW (1994) RBE-LET relationships for different types of lethal radiation damage in mammalian cells: comparison with DNA dsb and an interpretation of differences in radiosensitivity. *Int J Radiat Biol* 66:433–436
- Belloni F, Bettega D, Calzolari P, Cherubini R, Massariello P, Tallone L (2002) Inactivation cross sections for mammalian cells exposed to charged particles: a phenomenological approach. *Radiat Prot Dosimetry* 99:199–202
- Bisby RH, Cundall RB, Movassaghi S, Adams GE, Posener ML, Wardman P (1982) Selective free radical reactions with proteins and enzymes: a reversible equilibrium in the reaction of (SCN)<sub>2</sub> radical with lysozyme. *Int J Radiat Biol Relat Stud Phys Chem Med* 42:163–171
- Bisby RH, Cundall RB, Sims HE, Burns WG (1984) The inactivation of papain by high LET radiations. *Int J Radiat Biol Relat Stud Phys Chem Med* 46:261–268
- Blasius M, Sommer S, Hubscher U (2008) *Deinococcus radiodurans*: what belongs to the survival kit? *Crit Rev Biochem Mol Biol* 43:221–238
- Butts JJ, Katz R (1967) Theory of RBE for heavy ion bombardment of dry enzymes and viruses. *Radiat Res* 30:855–871
- Culard F, Gervais A, de Vuyst G, Spotheim-Maurizot M, Charlier M (2003) Response of a DNA-binding protein to radiation-induced oxidative stress. *J Mol Biol* 328:1185–1195
- Culard F, Bouffard S, Charlier M (2005) High-LET irradiation of a DNA-binding protein: protein-protein and DNA-protein cross-links. *Radiat Res* 164:774–780
- D'Souza DI, Harrison L (2003) Repair of clustered uracil DNA damages in *Escherichia coli*. *Nucleic Acids Res* 31:4573–4581
- Daly MJ (2006) Modulating radiation resistance: Insights based on defenses against reactive oxygen species in the radioresistant bacterium *Deinococcus radiodurans*. *Clin Lab Med* 26:491–504
- Daly MJ (2009) A new perspective on radiation resistance based on *Deinococcus radiodurans*. *Nat Rev Microbiol* 7:237–245
- Daly MJ, Gaidamakova EK, Matrosova VY, Vasilenko A, Zhai M, Venkateswaran A, Hess M, Omelchenko MV, Kostandarithes HM, Makarova KS, Wackett LP, Fredrickson JK, Ghosal D

- (2004) Accumulation of Mn(II) in *Deinococcus radiodurans* facilitates gamma-radiation resistance. *Science* 306:1025–1028
- Daly MJ, Gaidamakova EK, Matrosova VY, Vasilenko A, Zhai M, Leapman RD, Lai B, Ravel B, Li SM, Kemner KM, Fredrickson JK (2007) Protein oxidation implicated as the primary determinant of bacterial radioresistance. *PLoS Biol* 5:e92
- Dewey DL (1969) The survival of *Micrococcus radiodurans* irradiated at high LET and the effect of acridine orange. *Int J Radiat Biol Relat Stud Phys Chem Med* 16:583–592
- Eon S, Culard F, Sy D, Charlier M, Spotheim-Maurizot M (2001) Radiation disrupts protein-DNA complexes through damage to the protein. The lac repressor-operator system. *Radiat Res* 156:110–117
- Ghosal D, Omelchenko MV, Gaidamakova EK, Matrosova VY, Vasilenko A, Venkateswaran A, Zhai M, Kostandarithes HM, Brim H, Makarova KS, Wackett LP, Fredrickson JK, Daly MJ (2005) How radiation kills cells: survival of *Deinococcus radiodurans* and *Shewanella oneidensis* under oxidative stress. *FEMS Microbiol Rev* 29:361–375
- Gillard N, Begusova M, Castaing B, Spotheim-Maurizot M (2004) Radiation affects binding of Fpg repair protein to an abasic site containing DNA. *Radiat Res* 162:566–571
- Gillard N, Goffinont S, Bure C, Davidkova M, Maurizot JC, Cadene M, Spotheim-Maurizot M (2007) Radiation-induced oxidative damage to the DNA-binding domain of the lactose repressor. *Biochem J* 403:463–472
- Goodhead DT (2006) Energy deposition stochastics and track structure: what about the target? *Radiat Prot Dosimetry* 122:3–15
- Goodhead DT, Nikjoo H (1987) Physical mechanism for inactivation of metallo-enzymes by characteristic X-rays: analysis of the data of Jawad and Watt. *Int J Radiat Biol Relat Stud Phys Chem Med* 52:651–658
- Hada M, Georgakilas AG (2008) Formation of clustered DNA damage after high-LET irradiation: a review. *J Radiat Res (Tokyo)* 49:203–210
- Hamada N, Funayama T, Wada S, Sakashita T, Kakizaki T, Ni M, Kobayashi Y (2006) LET-dependent survival of irradiated normal human fibroblasts and their descendants. *Radiat Res* 166:24–30
- Henriksen T (1966) Production of free radicals in solid biological substances by heavy ions. *Radiat Res* 27:676–693
- Hirayama R, Ito A, Tomita M, Tsukada T, Yatagai F, Noguchi M, Matsumoto Y, Kase Y, Ando K, Okayasu R, Furusawa Y (2009) Contributions of direct and indirect actions in cell killing by high-LET radiations. *Radiat Res* 171:212–218
- Imamura M, Sawada S, Kasahara-Imamura M, Harima K, Harada K (2002) Synergistic cell-killing effect of a combination of hyperthermia and heavy ion beam irradiation: in expectation of a breakthrough in the treatment of refractory cancers (review). *Int J Mol Med* 9:11–18
- Jonah CD, Madhava Rao BS (2001) Radiation chemistry: present status and future trends. Elsevier, Amsterdam
- Kiefer J, Egenolf R, Ikpeme SE (2002a) DNA double strand break induction in yeast. *Radiat Prot Dosimetry* 99:269–272
- Kiefer J, Egenolf R, Ikpeme S (2002b) Heavy ion-induced DNA double-strand breaks in yeast. *Radiat Res* 157:141–148
- Kowalczyk A, Serafin E, Puchala M (2008) Inactivation of chosen dehydrogenases by the products of water radiolysis and secondary albumin and haemoglobin radicals. *Int J Radiat Biol* 84:15–22
- Kreipl MS, Friedland W, Paretzke HG (2009) Time- and space-resolved Monte Carlo study of water radiolysis for photon, electron and ion irradiation. *Radiat Environ Biophys* 48:11–20
- Meesungnoen J, Jay-Gerin JP (2005) High-LET radiolysis of liquid water with  $^{1}\text{H}^{+}$ ,  $^{4}\text{He}^{2+}$ ,  $^{12}\text{C}^{6+}$ , and  $^{20}\text{Ne}^{9+}$  ions: effects of multiple ionization. *J Phys Chem A* 109:6406–6419
- Micke U, Horneck G, Kozubek S (1994) Double strand breaks in the DNA of *Bacillus subtilis* cells irradiated by heavy ions. *Adv Space Res* 14:207–211
- Montaner B, O'Donovan P, Reelfs O, Perrett CM, Zhang X, Xu YZ, Ren X, Macpherson P, Frith D, Karran P (2007) Reactive oxygen-mediated damage to a human DNA replication and repair protein. *EMBO Rep* 8:1074–1079
- Mozumder A (1999) Fundamentals of radiation chemistry. Academic Press, San Diego
- Pinto M, Prise KM, Michael BD (2002a) Double strand break rejoining after irradiation of human fibroblasts with X rays or alpha particles: PFGE studies and numerical models. *Radiat Prot Dosimetry* 99:133–136
- Pinto M, Prise KM, Michael BD (2002b) Quantification of radiation induced DNA double-strand breaks in human fibroblasts by PFGE: testing the applicability of random breakage models. *Int J Radiat Biol* 78:375–388
- Roots R, Chatterjee A, Chang P, Lommel L, Blakely EA (1985) Characterization of hydroxyl radical-induced damage after sparsely and densely ionizing irradiation. *Int J Radiat Biol Relat Stud Phys Chem Med* 47:157–166
- Roots R, Holley W, Chatterjee A, Irizarry M, Kraft G (1990) The formation of strand breaks in DNA after high-LET irradiation: a comparison of data from in vitro and cellular systems. *Int J Radiat Biol* 58:55–69
- Sagstuen E, Sanderud A, Hole EO (2004) The solid-state radiation chemistry of simple amino acids, revisited. *Radiat Res* 162:112–119
- Saha A, Mandal PC, Bhattacharyya SN (1992) Radiation-induced inactivation of dihydroorotate dehydrogenase in dilute aqueous solution. *Radiat Res* 132:7–12
- Schmid AK, Lidstrom ME (2002) Involvement of two putative alternative sigma factors in stress response of the radioresistant bacterium *Deinococcus radiodurans*. *J Bacteriol* 184:6182–6189
- Shuryak I, Brenner DJ (2009) A model of interactions between radiation-induced oxidative stress, protein and DNA damage in *Deinococcus radiodurans*. *J Theor Biol* 261:305–317
- Spinks JWT, Woods RJ (1990) An introduction to radiation chemistry. Wiley, New York
- Stadtman ER (1993) Oxidation of free amino acids and amino acid residues in proteins by radiolysis and by metal-catalyzed reactions. *Annu Rev Biochem* 62:797–821
- Stenerlow B, Hoglund E, Carlsson J (2002a) DNA fragmentation by charged particle tracks. *Adv Space Res* 30:859–863
- Stenerlow B, Hoglund E, Elmroth K, Karlsson KH, Radulescu I (2002b) Radiation quality dependence of DNA damage induction. *Radiat Prot Dosimetry* 99:137–141
- Sukhi SS, Shashidhar R, Kumar SA, Bandekar JR (2009) Radiation resistance of *Deinococcus radiodurans* R1 with respect to growth phase. *FEMS Microbiol Lett*
- Taguchi M, Kojima T (2005) Yield of OH radicals in water under high-density energy deposition by heavy-ion irradiation. *Radiat Res* 163:455–461
- Taguchi M, Kimura A, Watanabe R, Hirota K (2009) Estimation of yields of hydroxyl radicals in water under various energy heavy ions. *Radiat Res* 171:254–263
- Takahashi T, Yatagai F, Kitayama S (1983) Effect of heavy ions on bacterial spores. *Adv Space Res* 3:95–104
- Terato H, Tanaka R, Nakaarai Y, Hirayama R, Furusawa Y, Ide H (2007) Analysis of complex DNA lesions generated by heavy ion beams. *Nucleic Acids Symp Ser (Oxf)*: 221–222
- Tsuruoka C, Suzuki M, Kanai T, Fujitaka K (2005) LET and ion species dependence for cell killing in normal human skin fibroblasts. *Radiat Res* 163:494–500
- Ward JF (1990) The yield of DNA double-strand breaks produced intracellularly by ionizing radiation: a review. *Int J Radiat Biol* 57:1141–1150

- Xue L, Yu D, Furusawa Y, Okayasu R, Tong J, Cao J, Fan S (2009) Regulation of ATM in DNA double strand break repair accounts for the radiosensitivity in human cells exposed to high linear energy transfer ionizing radiation. *Mutat Res* 670:15–23
- Yamaguchi H, Uchihori Y, Yasuda N, Takada M, Kitamura H (2005) Estimation of yields of OH radicals in water irradiated by ionizing radiation. *J Radiat Res (Tokyo)* 46:333–341
- Yamamoto T, Matsumura A, Yamamoto K, Kumada H, Hori N, Torii Y, Shibata Y, Nose T (2003) Characterization of neutron beams for boron neutron capture therapy: in-air radiobiological dosimetry. *Radiat Res* 160:70–76
- Yamashita S, Katsumura Y, Lin M, Muroya Y, Miyazaki T, Murakami T, Meesungnoen J, Jay-Gerin JP (2008) Water radiolysis with heavy ions of energies up to 28 GeV. 3. Measurement of G(MV<sup>+</sup>) in deaerated methyl viologen solutions containing various concentrations of sodium formate and Monte Carlo simulation. *Radiat Res* 170:521–533
- Yang N, Chaudhry MA, Wallace SS (2006) Base excision repair by hNTH1 and hOGG1: a two edged sword in the processing of DNA damage in gamma-irradiated human cells. *DNA Repair (Amst)* 5:43–51
- Yokota Y, Yamada S, Hase Y, Shikazono N, Narumi I, Tanaka A, Inoue M (2007) Initial yields of DNA double-strand breaks and DNA fragmentation patterns depend on linear energy transfer in tobacco BY-2 protoplasts irradiated with helium, carbon and neon ions. *Radiat Res* 167:94–101
- Zahradka K, Slade D, Bailone A, Sommer S, Averbeck D, Petranovic M, Lindner AB, Radman M (2006) Reassembly of shattered chromosomes in *Deinococcus radiodurans*. *Nature* 443:569–573
- Zimmermann H, Schafer M, Schmitz C, Bucker H (1994) Effects of heavy ions on inactivation and DNA double strand breaks in *Deinococcus radiodurans* R1. *Adv Space Res* 14:213–216